

**H. J. Rathbun**

Mem. ASME

e-mail: palmtree@engineering.ucsb.edu

**Z. Wei**

**M. Y. He**

**F. W. Zok**

**A. G. Evans**

Mem. ASME

Materials and Mechanical Engineering  
Departments,  
University of California,  
Santa Barbara, CA 93106

**D. J. Sypeck**

Mem. ASME

Aerospace Engineering Department,  
Embry-Riddle Aeronautical University,  
Daytona Beach, FL 32114

**H. N. G. Wadley**

Department of Materials Science and  
Engineering,  
University of Virginia,  
Charlottesville, VA 22903-2442

# Measurement and Simulation of the Performance of a Lightweight Metallic Sandwich Structure With a Tetrahedral Truss Core

*Metallic sandwich panels with tetrahedral truss cores have been fabricated and their structural performance evaluated. A fabrication technique involving deformation-shaping and brazing has been used. The responses of the structure in core shear and panel bending have been measured. The results demonstrate robust behavior beyond the limit load. A finite element simulation of the core shear response duplicates the features found experimentally. When combined with the constitutive properties of the face sheet material, these shear characteristics have been shown to predict, with good fidelity, the limit load for panels in bending. [DOI: 10.1115/1.1757487]*

## 1 Introduction

The attainment of minimum weight structures has a long history, [1–8]. Three technical factors are involved in achieving this goal: (i) materials selection, [1], (ii) topology optimization, [9–17], and (iii) multifunctionality, [12,16]. Topologies that can be used to achieve high load capacity at low weight are exemplified by truss structures that stretch or compress without bending and honeycomb core panels, [11–20]. The truss topology has the benefit that the open spaces can be used to impart functionalities in addition to load bearing, such as active cooling [1,12,16], whereupon, the extra weight of an additional component normally needed to imbue that extra function can be saved.

Performance indices are needed to ascertain minimum weight configurations and to compare designs. The indices are based on overall structural weight,  $W$  (per unit area), load,  $P$  (per unit width), stiffness, and yield strain,  $\varepsilon_Y$ . When the faces and the core are made from the same alloy, the weight index is, [1,6,11]:

$$\Psi = \frac{W}{\rho L} \quad (1)$$

where  $L$  is the length of the panel/beam and  $\rho$  the density of the solid material.

For designs based on *strength*, the loads supported in *compression* can be compared using the load index, [6]:

$$\Pi = \frac{P}{EL} \quad (2a)$$

where  $E$  is the Young's modulus. For *bending* over a span  $S$ , it is more convenient to express the load index through a combination of the maximum bending moment,  $M$ , and maximum transverse shear,  $V$  (both per unit width), [11]:

$$\Pi_b = \frac{V}{\sqrt{EM}} \quad (2b)$$

The ratio of the maximum  $M$  and  $V$  defines a characteristic length scale,  $\ell \equiv M/V$ , [11]. For example, in three-point bending,  $\ell = S/2$ , [11,17]. When this index is used, the weight index (1) is redefined with  $\ell$  replacing  $L$ .

Comparative indices exist for *stiffness* but they are configuration-dependent, [1,2,7,9]. Stiffness governs the weight at smaller loads, while strength is performance limiting at higher loads, [1], exemplified by Fig. 1. The present assessment is restricted to strength-limited designs, pertinent to high loads.

Strength-limited minimum weight designs are found by *identifying the failure modes*, specifying the load capacity and then varying the dimensions to determine the lowest weight for each mode, [1,11]. The benchmark configurations against which competing technologies should be compared are summarized on Fig. 2, [12,15].

For flat panels, sandwich designs with honeycomb cores represent the performance benchmark in bending [11] (Fig. 2(a)), while hat-stiffened panels define the benchmark in compression, [6], (Fig. 2(b)). For curved configurations, the reference system is comprised of distributed axial and circumferential stiffeners, [1,12,21], (Fig. 2(c)). Alternative topologies need not structurally outperform these benchmarks, provided that they exploit other attributes such as cost, durability, strength retention after impact, [1,22,23], and multifunctionality, [1,12,16].

Contributed by the Applied Mechanics Division of THE AMERICAN SOCIETY OF MECHANICAL ENGINEERS for publication in the ASME JOURNAL OF APPLIED MECHANICS. Manuscript received by the ASME Applied Mechanics Division, December 2, 2002; final revision, December 29, 2003. Associate Editor: E. Arruda. Discussion on the paper should be addressed to the Editor, Prof. Robert M. McMeeking, Journal of Applied Mechanics, Department of Mechanical and Environmental Engineering, University of California–Santa Barbara, Santa Barbara, CA 93106-5070, and will be accepted until four months after final publication of the paper itself in the ASME JOURNAL OF APPLIED MECHANICS.

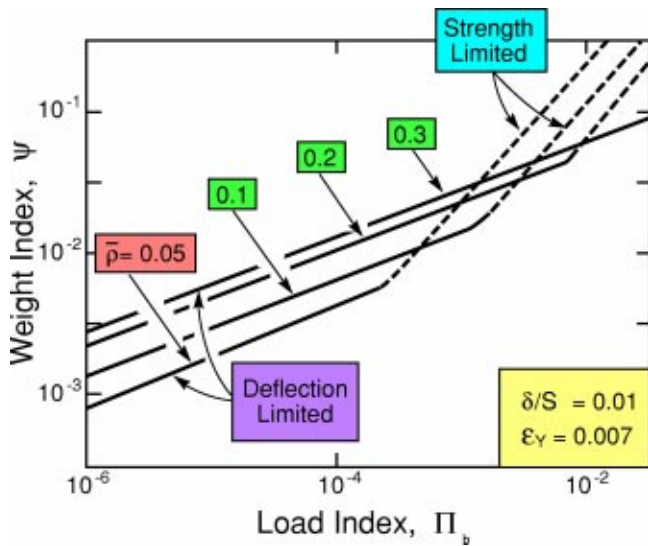


Fig. 1 The minimum weight as a function of load for a simply supported panel subject to a uniformly distributed pressure, evaluated for a material with yield strain,  $\epsilon_{\gamma}=0.007$ , and maximum allowable center displacement,  $\delta/S=0.1$ . Results are presented for several values of the relative density of the core. In all cases, at large loads, the panels become strength-limited.

Panels with open truss cores offer one such alternative, [11,18]. They are more amenable to forming into complex shapes than honeycomb cores, [19], and they allow fluids to readily pass through, [16], rendering them less susceptible to internal corrosion. They are also attractive for cross flow heat exchange, [7]. In flat panels, when optimized, such cores are as light as the benchmark designs in both bending, [11], (Fig. 2(a)) and compression, [1,21], (Fig. 2(b)). Moreover, in curved panels, they are much more structurally efficient than stiffened designs, [1,21], (Fig. 2(c)). At loads relevant to aerospace applications, [6], the minimum weight occurs at a core relative density in the range 2–3%, with thin faces (thickness to load span of order  $3 \times 10^{-3}$ ), [11]. The failure mechanisms operating at the optimum depend on the yield strain of the alloy being used, [11]. At the high yield strains pertinent to aerospace grade Al alloys, failure occurs by concurrent face yielding, face buckling and elastic buckling of the compressed truss core members, [11]. For the lower yield strains relevant to stainless steels, the failure modes are concurrent face yielding, face buckling and core member yielding, [11].

Experimental assessments of these predictions have been made in panels fabricated by an investment casting process, [18], using materials having yield strains in the range where the core response is yield (rather than elastic buckling) dominated. These investigations had two primary limitations: (i) due to the constraints on aspect ratio imposed by investment casting, the core members were less slender than that at the optimum, (ii) the casting introduced defects that limited the ductility, inhibiting the ability to probe the performance envelope. Other limitations included the relatively high manufacturing cost associated with investment casting, as well as the limited property range that can be accessed (relative to wrought material).

These issues are addressed in the present study by applying a manufacturing procedure for open cell tetrahedral truss core structures (Fig. 3) applicable to wrought metals, [19]. The cores are made using metal perforation and deformation-shaping processes. They are bonded to thin metal face sheets using a brazing approach. The specific objectives of this article are as follows: (i) manufacture wrought panels with core densities in the range found for fully optimized panels (about 2%), [11]; (ii) measure the performance of these panels subject to overall bending loads, as-

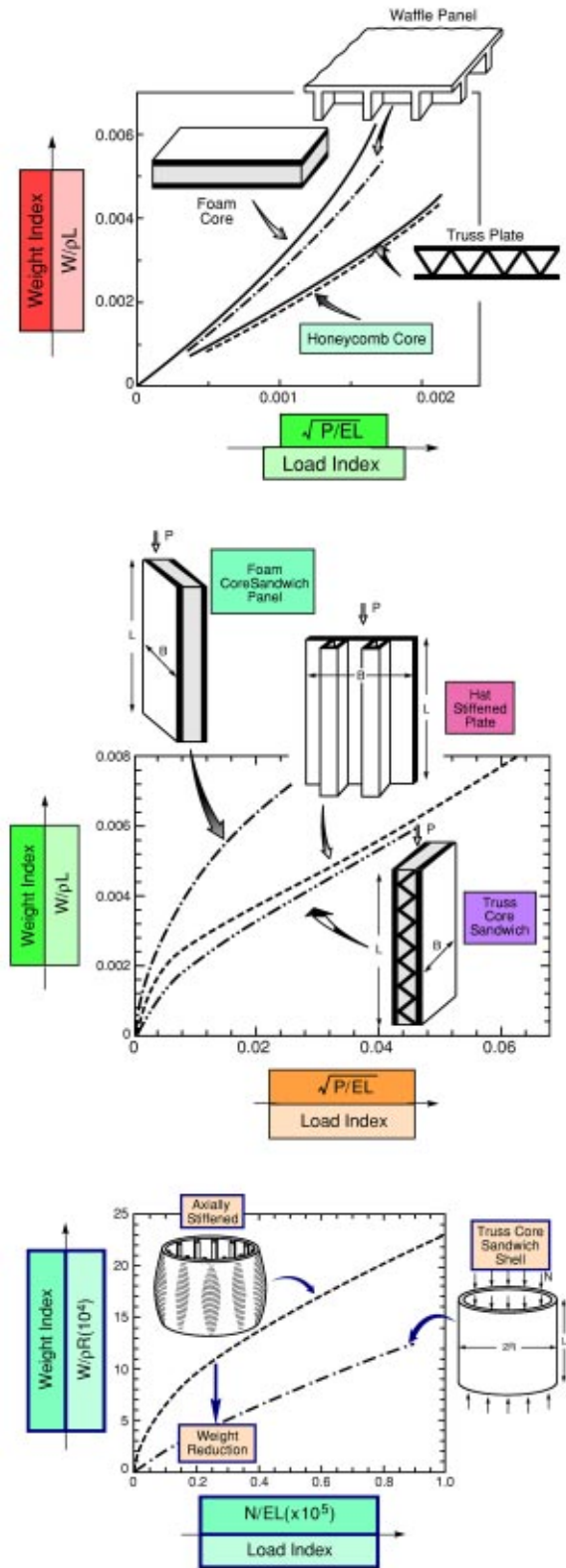


Fig. 2 (a) The minimum weight as a function of load capacity for various panels under shear and bending load. (b) Weight index versus load index for axially compressed flat panels, [1,10,18,22]. (c) The minimum weight as a function of load for axially compressed curved panels.  $N$  is the load per unit length of the periphery, [12].

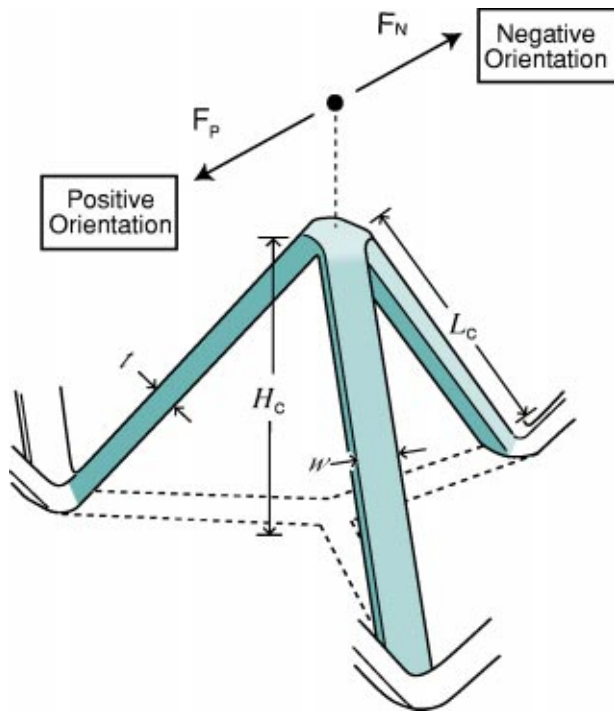


Fig. 3 Tetrahedral unit with ligaments having rectangular cross-section. The directions of positive and negative shear are indicated.

sess their robustness, and compare the load capacity with predictions, [11]; (iii) perform independent core shear measurements and simulations to facilitate model validation.

## 2 Basic Mechanics

The four possible failure modes for the tetrahedral truss core sandwich structure with solid face sheets are face sheet yielding, face sheet buckling, core member yielding and core member buckling, [11]. The face sheet failure modes are dictated by the bending moment per unit width,  $M$ . The associated constraints are, [11]:

$$\frac{M}{t_f H_c} \leq \sigma_y \quad (\text{face sheet yielding}) \quad (3a)$$

$$\frac{M}{t_f H_c} \leq \frac{49\pi^2 E}{432(1-\nu^2)} \left(\frac{t_f}{d}\right)^2 \quad (\text{face sheet buckling}) \quad (3b)$$

where  $H_c$  is the core height,  $t_f$  is the face sheet thickness,  $L_c$  is the truss member length,  $d = \sqrt{L_c^2 - H_c^2}$ ,  $\sigma_y$  is the yield strength, and  $\nu$  is Poisson's ratio. The core failure modes are dictated by the shear force per unit width,  $V$ , [11]. For truss members with rectangular cross-section (width,  $w$  and thickness,  $t$ ), the constraints are

$$\frac{\sqrt{3} V d L_c}{H_c w t} \leq \sigma_y \quad (\text{core member yielding}) \quad (3c)$$

$$\frac{\sqrt{3} V d L_c}{H_c w t} \leq \frac{k \pi^2 E}{12} \left(\frac{t}{L_c}\right)^2 \quad (\text{core member buckling}) \quad (3d)$$

where  $k$  depends on the end conditions of the truss members. For conservatism, we assume that the nodal connections between the core members and the face sheets are pin-jointed ( $k=1$ ), [11]. For convenience, each geometric parameter is normalized by  $\ell$ , allowing the constraint functions to be rewritten in the nondimensional forms:

$$\left(\frac{V}{\sqrt{EM}}\right)^2 \frac{E}{\sigma_y} \frac{\ell^2}{t_f H_c} \leq 1 \quad (\text{face sheet yielding}) \quad (4a)$$

$$\left(\frac{V}{\sqrt{EM}}\right)^2 \frac{432(1-\nu^2)}{49\pi^2} \frac{d^2 \ell^2}{t_f^3 H_c} \leq 1 \quad (\text{face sheet buckling}) \quad (4b)$$

$$\left(\frac{V}{\sqrt{EM}}\right)^2 \frac{E}{\sigma_y} \frac{\sqrt{3} d L_c \ell}{H_c w t} \leq 1 \quad (\text{core member yielding}) \quad (4c)$$

$$\left(\frac{V}{\sqrt{EM}}\right)^2 \frac{12\sqrt{3}}{k\pi^2} \frac{d L_c^3 \ell}{H_c w t^3} \leq 1 \quad (\text{core member buckling}) \quad (4d)$$

A failure mode is considered active when the associated constraint function reaches unity. As discussed below (Section 6), this approach can be used to predict the load at failure initiation during panel bending.

## 3 Sandwich Panel Construction

Truss cores can be fabricated from wrought metals by starting with perforated metal sheets and bending along diagonal nodes, [19]. To illustrate the fabrication, commercially available 304 stainless steel (Fe-18Cr-8Ni) with hexagonal perforations was obtained from Woven Metal Products, Inc. (Alvin, TX). The truss members had width  $w = 1.26$  mm and thickness,  $t = 0.59$  mm. The rectangular cross sections (which have lower core performance than square sections) were convenient for manufacturing, [19]. After bending (Fig. 4(a)), the core height was,  $H_c = 10$  mm, such

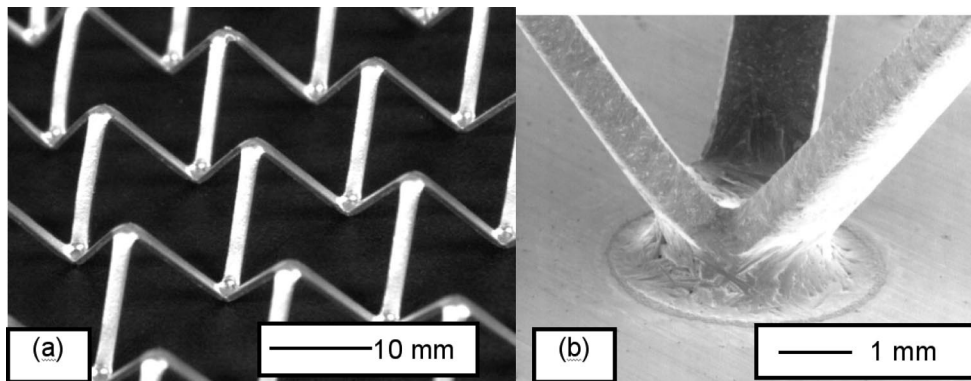


Fig. 4 (a) Tetrahedral truss core after shaping, (b) typical core/face sheet bond

**Table 1 Geometric parameters for three point bending panels**

| Parameter                   | Dimension (mm) |
|-----------------------------|----------------|
| Core height, $H_c$          | 9.8            |
| Face sheet thickness, $t_f$ | 0.75           |
| Truss member length, $L_c$  | 12.2           |
| Truss member width, $w$     | 1.26           |
| Truss member thickness, $t$ | 0.59           |
| Span length, $S$            | 202            |
| Panel width, $B$            | 66             |

that the relative density was,  $\bar{\rho} \equiv \rho_c / \rho = 1.7\%$ , (where  $\rho_c$  is the density of the core and  $\rho$  is the density of the solid material).

A brazing approach was used for attaching the face-sheets to the cores. The cores were lightly sprayed with a powder comprising a mix of a polymer (Nicrobraz® 520) and 140 mesh Ni-25Cr-10P alloy (Nicrobraz® 51), both supplied by Wal Colmonoy Corp. (Madison Heights, MI). The solidus and liquidus of this alloy are 880 and 950°C, respectively, whereas the solidus of 304 stainless steel is approximately 1400°C. The coated cores were placed between solid 304 stainless steel face sheets and a small compressive pressure was applied. The panel assemblies were heated in vacuum ( $< 10^{-2}$  torr) to 550°C for 1h to volatilize the polymer<sup>1</sup>. The system was evacuated to less than  $10^{-3}$  torr, and the temperature increased to 1100°C and held for 1 h. At temperature, the alloy melts and is drawn into the core/face sheet contacts by capillarity. Bonding then occurs as interdiffusion changes the local composition, causing it to solidify. Robust joints with desirable nodes ensue (Fig. 4(b)). Upon bonding, the core height diminishes slightly, to  $H_c = 9.8$  mm, increasing the core relative density to  $\bar{\rho} = 1.8\%$ . This density is very close to that found for fully optimized panels, [11].

For the panel bending assessment, a face sheet thickness,  $t_f = 0.75$  mm, was chosen, exceeding that for the optimum structure, [11]. For the core shear tests, much thicker face sheets were used ( $t_f = 3$  mm) to prevent distortions during the measurements.

#### 4 Test Design

After cooling to ambient, the panels were machined for testing. The flexure panels had span length,  $S = 202$  mm, width  $B = 66$  mm, and mass 0.22 kg (Table 1). They were tested in three-point loading by using a procedure similar to that described elsewhere, [19,22]. Flat-faced loading platens 16 mm thick were adhesively bonded to the faces of the panels. The loads were applied through lubricated rollers inset into the platens that allowed the specimen to rotate upon bending, with minimal friction. The tests were performed in a servo-electric test frame. The load and load-point displacements were measured simultaneously.

The shear test assembly comprised two L-shaped platens that rigidly held each of the two face sheets of the panel (Fig. 5). The assembly was placed between flat loading surfaces connected to the load cell and actuator of a servo-hydraulic load frame. Imposing a compressive load to the assembly created a condition of nearly pure shear at the truss core. The tests were performed at a load point displacement rate of 0.1 mm/min. Displacements were measured by a laser extensometer. Tests were performed in the negative and positive orientations shown in Fig. 3, [18,20]. In the positive orientation, one truss member is in tension and the other two in compression and vice versa for the negative orientation.

A high resolution digital camera was connected to the testing frame in order to capture side-view images of the core. These images were used to identify the failure mechanisms.

The constitutive properties of the 304 stainless steel used in the face sheets were measured after exposure to a simulated bonding cycle (1100°C for one hour). Flat dog-bone-shaped tensile specimens were tested at a strain rate of  $10^{-4} \text{ s}^{-1}$ .

<sup>1</sup>Note that the alloy powder remains adhered to the structure after volatilization.

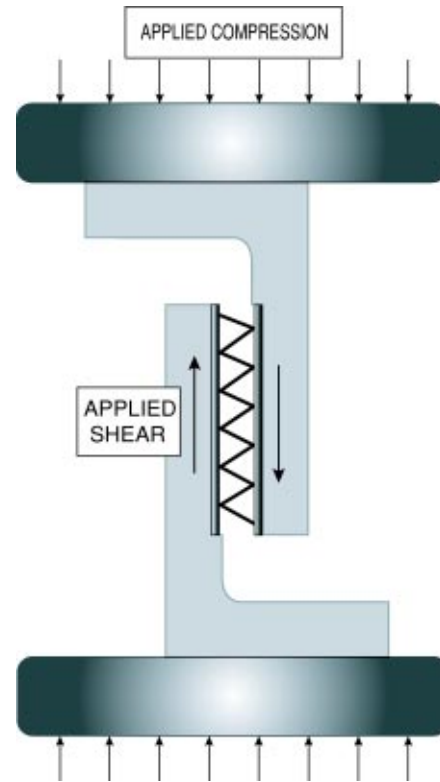


**Fig. 5 Shear test fixture assembly**

#### 5 Measurements and Observations

Figure 6 shows the true stress-strain response of the 304 stainless steel. The material exhibits a 0.2% offset yield strength,  $\sigma_y = 217$  MPa. The hardening rate beyond yield is almost linear up to a strain of 10% and can be characterized by a hardening modulus,  $H \equiv d\sigma/d\epsilon = 2.5$  GPa.

The shear stress/strain responses measured in the positive and negative orientations (Fig. 7) demonstrate the asymmetry of the tetrahedral truss core. In the negative orientation, the limit load is

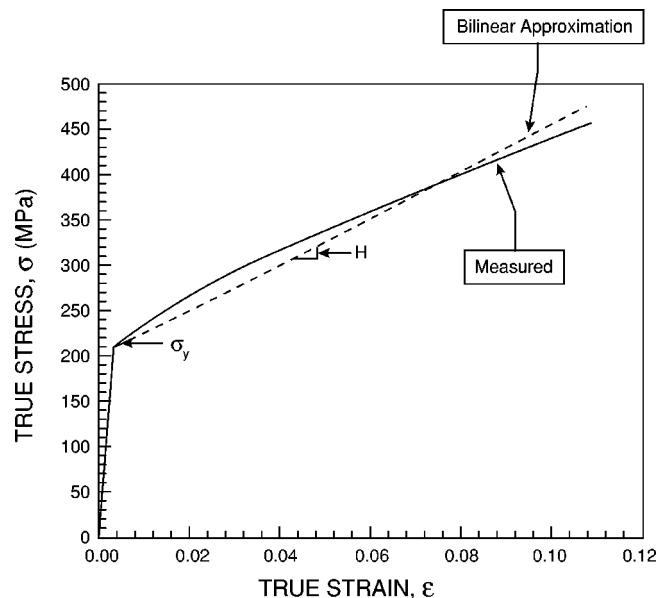


**Fig. 6 True stress-strain response for 304 stainless steel following annealing at 1100°C for 1 hour**

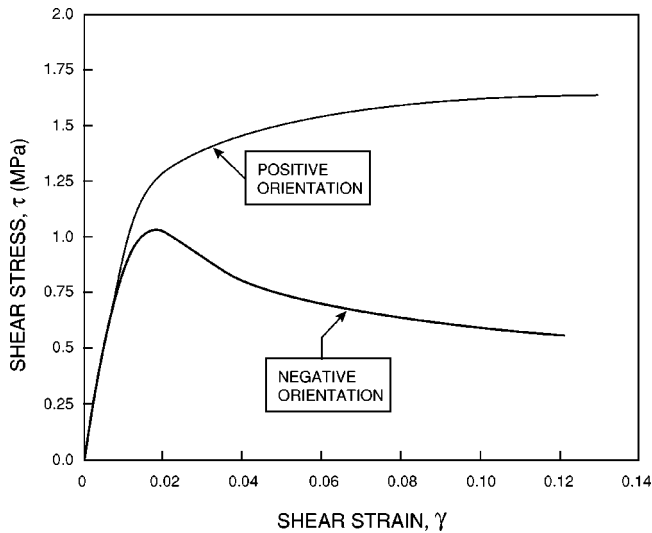


Fig. 7 Shear stress/strain response of tetrahedral truss core panels in the negative and positive orientations

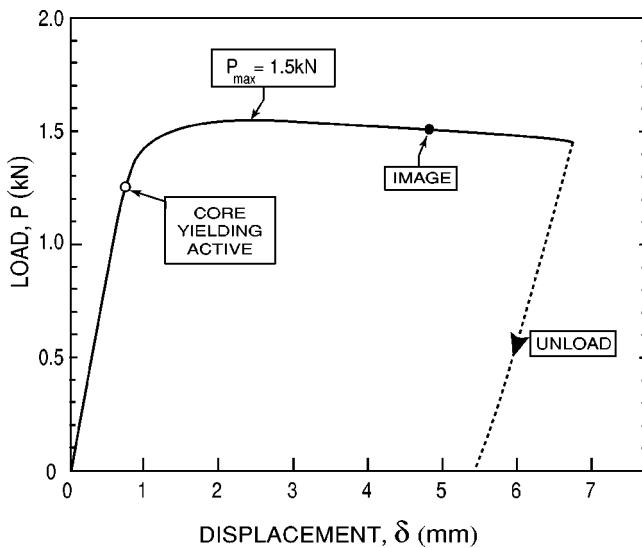


Fig. 8 Load-deflection response during panel bending. The open symbol represents the predicted load from Eq. (5) at which yielding occurs.

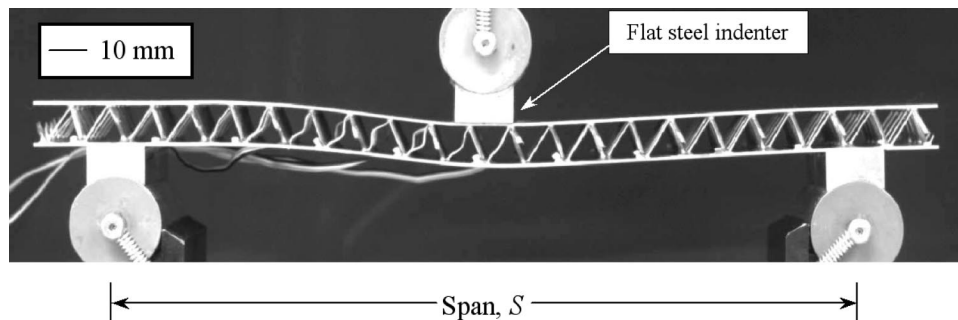


Fig. 9 Image of the panel obtained at the displacement indicated in Fig. 8. Note the plastic buckling of the compressed truss core members on the left side and the associated plastic hinge. The span  $S=202$  mm, the flat steel indenters were 16.0 mm wide and the overhang,  $h_{\text{over}}=22.5$  mm.

appreciably lower than in the positive orientation because the most heavily stressed trusses are in compression and susceptible to plastic buckling, [18,20]. The maximum shear stress in this orientation,  $\tau_{\text{max}}=1.0$  MPa, occurs at a shear strain of 1.4%, observed to be coincident with plastic buckling of the compressed members. In the positive orientation, the corresponding maximum is  $\tau_{\text{max}}=1.7$  MPa, occurring at a shear strain of 13%. In this orientation, the most highly stressed trusses are in tension. They stretch and transfer load onto the compressed trusses, eventually causing them to buckle plastically.

A load/displacement curve measured in bending is summarized in Fig. 8. An approximately steady-state load,  $P_{ss}=1.5$  kN is attained at displacements between  $2 \text{ mm} < \delta_{ss} < 5 \text{ mm}$ , followed by gradual softening beyond 5 mm. An image obtained at the limit load (Fig. 9) indicates that the response is asymmetric and that the panel fails by core shear. That is, since the truss assemblies on the left experience shear in the negative orientation, [18], failure occurs through plastic buckling of the compressed members. The buckling induces large strains that cause face sheet yielding and result in the formation of a macroscopic plastic hinge at the outer loading platen, [1,20,22]. In contrast, the right side experiences positive shear. Consequently, the trusses stretch with relatively small ensuing strain levels, inhibiting both face yielding and hinging. After unloading, all of the core/face-sheet bonds were intact with no visible cracking.

## 6 Finite Element Simulation of the Shear Response

The finite element simulation approach is similar to that described by Hyun et al. [20]. The exact rectangular geometry of the truss members has been used, as well as the measured stress/strain curve for the faces (Fig. 6). The truss assembly and the finite element mesh are shown in Fig. 10. The finite element code ABAQUS has been used. The base of the truss assembly is fixed. The top, where the assembly is bonded to the upper face, is displaced parallel to the face, without rotation. The deformations of the core that occur in the negative and positive orientations at large displacements are shown in Fig. 10. They demonstrate the plastic buckling of the compressed member in the negative orientation and the stretching of the tensile member in the positive orientation.

The shear stress/plastic strain relations calculated for the two orientations are superposed on the experimental measurements in Fig. 11. The similarity between the curves in both orientations affirms the self-consistency of the present measurement and simulation protocols and provides confidence in the scaling relations (with relative density and core member aspect ratio) elaborated elsewhere, [11,13,20]. There are two minor discrepancies. The simulations generally underestimate the flow strength by a few percent. Since the simulations use the stiffest possible boundary

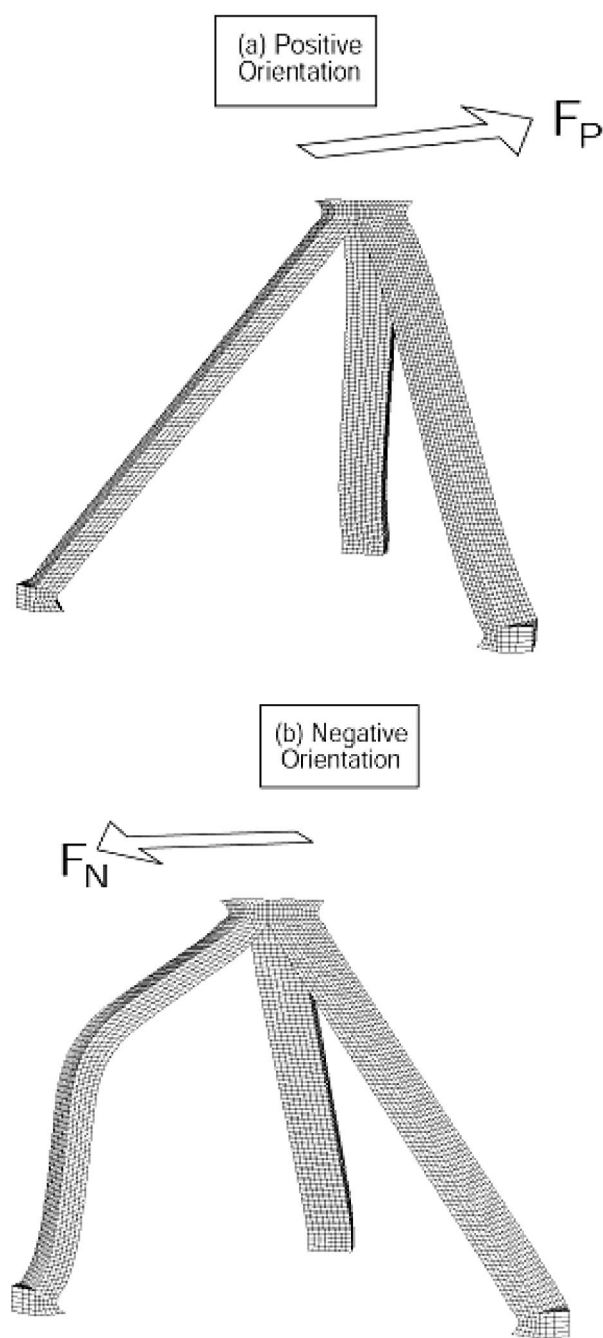


Fig. 10 Finite element simulations showing the deformation after shearing in (a) the positive orientation at  $\gamma_{pl}=0.14$  and (b) the negative orientation at  $\gamma_{pl}=0.10$ . Note the plastic buckling of the compressed member in the latter.

conditions, this difference implies that the material comprising the truss members has higher strain hardening than that measured for the faces. This may be attributable to chemical interactions between the braze alloy and the steel. The second discrepancy relates to the onset of plastic buckling in the negative orientation. The simulation overestimates the stress at which this occurs by about 10%. This difference is associated with the imperfection sensitivity of the buckling condition.

## 7 The Bending Response

**Initial Failure Load.** By inserting the geometric parameters for the panel (Table 1) into equation (4),<sup>2</sup> core member yielding is

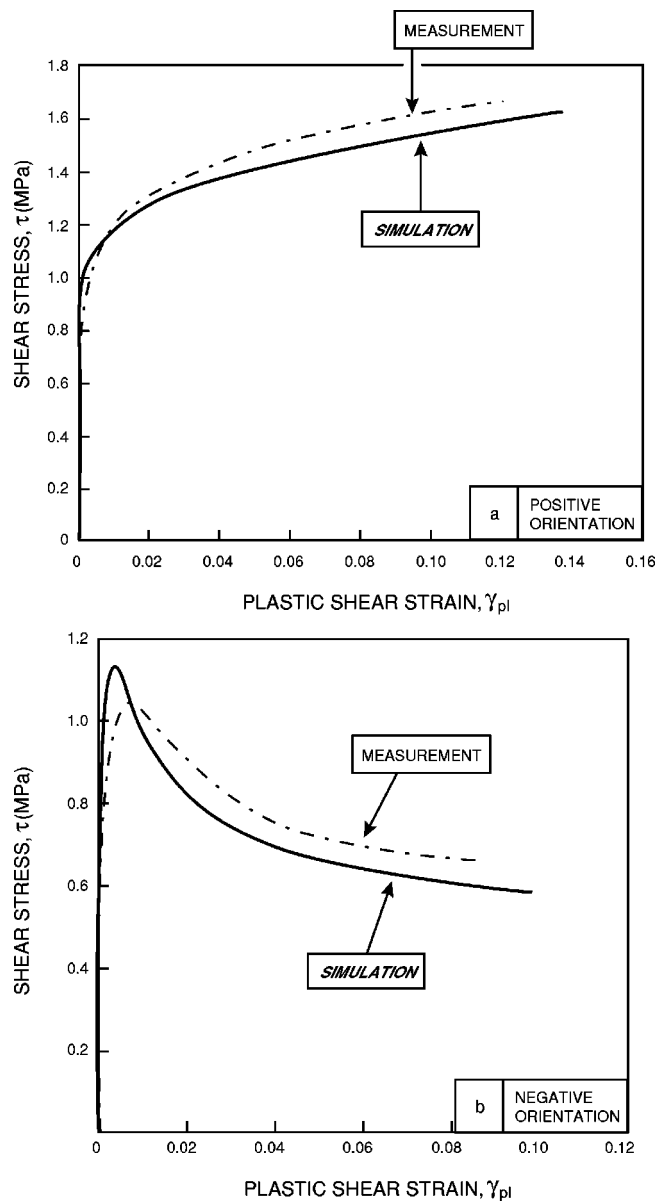


Fig. 11 Simulations of the shear stress as a function of plastic strain in (a) the positive orientation and (b) the negative orientation. The experimental measurements have been superposed.

found to become active at the lowest load, when  $\Pi_b \equiv V/\sqrt{EM} = 6.8 \times 10^{-4}$ . The corresponding absolute yield load is

$$P_y = \Pi_b^2 BES. \quad (5)$$

Inserting the panel dimensions (Table 1) into (5), the predicted yield load becomes  $P_y = 1.25$  kN. This value corresponds closely to that measured at the onset of nonlinearity (Fig. 8), affirming that failure initiates in the core.

**Limit Load.** The beam theory solution for the collapse load of a sandwich panel in three-point bending with small overhang,  $h_{over}$ , is given by, [1,22],

<sup>2</sup>The analysis assumes  $\sigma_y/E=0.001$  and  $\nu=0.33$ . Further, for three point bending,  $\ell=S/2=101$  mm.

$$P_A = \frac{2Bt_f^2}{S} \sigma_y + 2BH_c \tau_{\max} \left( 1 + \frac{2h}{S} \right). \quad (6a)$$

The corresponding result for a panel with large overhang is, [1,22],

$$P_B = \frac{2Bt_f^2}{S} \sigma_y + 2BH_c \tau_{\max}. \quad (6b)$$

Here, the pertinent value of  $\tau_{\max}$  is that corresponding to the softer, negative orientation. The lower of the two loads,  $P_A$  and  $P_B$ , dictates panel bending strength.

Upon incorporating into (6) the measured shear strength in the negative orientation,  $\tau_{\max} = 1.0$  MPa, the face sheet yield strength,  $\sigma_y = 217$  MPa, and the panel dimensions (Table 1), the peak loads are predicted to be  $P_A = 1.7$  kN and  $P_B = 1.5$  kN. The lower value is virtually identical to the measured collapse load. The quality of the agreement suggests that simple beam theory models can adequately account for measured limit loads, provided that independent information about the core shear strength and face strength is available.

## 8 Summary

Metallic sandwich panels with tetrahedral truss cores have been fabricated by deformation shaping and brazing. The responses in core shear and panel bending have been measured. The results demonstrate a robustness attributed to the wrought nature of the material. Finite element models of the shear response duplicate the essential features found experimentally. A small (few percent) discrepancy is attributed to incomplete understanding of the stress/strain characteristics of the material state in the truss members.

When combined with the constitutive properties of the face sheet material, the core shear characteristics have been used to predict the limit load for panels in bending by beam theory. The closeness of the agreement indicates that such models are capable of adequately predicting limit loads, given independent information about the core shear strength.

## Acknowledgments

We are grateful to DARPA/ONR for the support of this work through research grants N00014-96-1-1028 (program manager, S. Fishman) and N00014-01-1-0517 (program managers, L. Christodoulou and S. Fishman). Also, we would like to thank S. Chiras for performing the three-point bending experiment, and A. Jamieson for assistance in preparation of the figures.

## Nomenclature

|                   |   |
|-------------------|---|
| $B$               | = beam width  |
| $d$               | = base leg of tetrahedral truss assembly<br>( $\equiv \sqrt{L_c^2 - H_c^2}$ ) |
| $E$               | = Young's modulus   |
| $F_N$             | = shear force in negative orientation   |
| $F_P$             | = shear force in positive orientation   |
| $h_{\text{over}}$ | = overhang in three-point bend experiment                                     |
| $H$               | = hardening modulus   |
| $H_c$             | = core height   |
| $k$               | = buckling constant ( $k=1$ for pinned ends, $4$ for built-in ends)           |
| $L$               | = length of panel/beam  |
| $L_c$             | = truss member length   |
| $M$               | = moment per unit width   |
| $N$               | = load per unit peripheral length for axially compressed curved panels        |
| $P$               | = load per unit width   |
| $P_A, P_B$        | = collapse loads in bending for small and large overhangs, respectively       |
| $P_{ss}$          | = steady-state load in three-point bending                                    |

|                       |   |
|-----------------------|---|
| $P_y$                 | = yield load in three-point bending                   |
| $S$                   | = three-point bend span length                        |
| $t$                   | = truss core member thickness                         |
| $t_f$                 | = face sheet thickness                                |
| $V$                   | = shear per unit width                                |
| $w$                   | = truss core member width                             |
| $W$                   | = weight per unit area                                |
| $\delta$              | = displacement in three point bending                 |
| $\delta_{ss}$         | = deflection range for $P_{ss}$                       |
| $\epsilon_y$          | = yield strain  |
| $\gamma, \gamma_{pl}$ | = shear strain and plastic shear strain, respectively |
| $\ell$                | = characteristic length scale ( $\equiv M/V$ )        |
| $\Psi$                | = nondimensional weight index                         |
| $\Pi, \Pi_b$          | = load indices  |
| $\rho$                | = density of solid material                           |
| $\bar{\rho}$          | = relative core density ( $\equiv \rho_c / \rho$ )    |
| $\rho_c$              | = density of core                                     |
| $\sigma_y$            | = 0.2% offset yield strength                          |
| $\tau$                | = shear stress  |
| $\tau_{\max}$         | = maximum shear stress                                |
| $\nu$                 | = Poisson's ratio                                     |

## References

- [1] Ashby, M. F., Evans, A. G., Fleck, N. A., Gibson, L. J., Hutchinson, J. W., and Wadley, H. N. G., 2000, *Metal Foams: A Design Guide*, Butterworth-Heinemann, Boston, MA.
- [2] Clark, J. P., Roth, R., and Field, F. R., 1997, *Techno-Economic Issues in Material Science* (ASM Handbook Vol. 20, Materials Science and Design), ASM International, Materials Park, OH.
- [3] Allen, H. G., 1969, *Analysis and Design of Structural Sandwich Panels*, Pergamon Press, Oxford, UK.
- [4] Koiter, W. T., 1963, Koninkl. Nederl. Akademie van Wetenschappen, Ser. B, **66**, pp. 265–279.
- [5] Hutchinson, J. W., "Plastic Buckling," 1974, *Adv. Appl. Mech.*, **14**, pp. 67–144.
- [6] Budiansky, B., 1999, "On The Minimum Weights of Compression Structures," *Int. J. Solids Struct.*, **36**, pp. 3677–3708.
- [7] Gerard, G., 1956, *Minimum Weight Analysis of Compression Structures*, New York University Press, New York.
- [8] Tvergaard, V., 1973, "Imperfection-Sensitivity of a Wide Integrally Stiffened Panel Under Compression," *Int. J. Solids Struct.*, **9**, pp. 177–192.
- [9] Weaver, P. M., and Ashby, M. F., 1997, "Material Limits For Shape Efficiency," *Prog. Mater. Sci.*, **41**, pp. 61–128.
- [10] Parkhouse, J. G., 1984, *Structuring: A Process of Material Distribution*, *Proc. 3rd Int. Conf. On Space Structures*, H. Nooschin, ed., Elsevier, London, pp. 367–374.
- [11] Wicks, N., and Hutchinson, J. W., 2001, "Optimal Truss Plates," *Int. J. Solids Struct.*, **38**, pp. 5165–5183.
- [12] Evans, A. G., Hutchinson, J. W., Fleck, N. A., Ashby, M. F., and Wadley, H. N. G., 2001, "The Topological Design of Multifunctional Cellular Materials," *Prog. Mater. Sci.*, **46**, pp. 309–327.
- [13] Deshpande, V. S., and Fleck, N. A., 2001, "Collapse of Truss Core Sandwich Beams in 3-Point Bending," *Int. J. Solids Struct.*, **38**, pp. 6275–6305.
- [14] Fuller, R. B., 1961, "Synergetic Building Construction," U.S. Patent, 2,986,241, 30.
- [15] Evans, A. G., 2001, "Lightweight Materials and Structures," *MRS Bull.*, **26**, p. 790.
- [16] Gu, S., Lu, T. J., and Evans, A. G., 2001, "On The Design of Two-Dimensional Cellular Metals For Combined Heat Dissipation and Structural Load Capacity," *Int. J. Heat Mass Transfer*, **44**, pp. 2163–2175.
- [17] Zok, F. W., Rathbun, H. J., Wei, Z., and Evans, A. G., 2003, "Design of Metallic Textile Core Sandwich Panels," *Int. J. Solids Struct.*, **40**, pp. 5707–5722.
- [18] Chiras, S., Mumm, D. R., Evans, A. G., Wicks, N., Hutchinson, J. W., Dharmasena, K., Wadley, H. N. G., and Fichter, S., 2002, "The Structural Performance of Near-Optimized Truss Core Panels," *Int. J. Solids Struct.*, **39**, pp. 4093–4115.
- [19] Sypeck, D. J., and Wadley, H. N. G., 2002, "Cellular Metal Truss Core Sandwich Structures," *Advanced Engineering Materials*, **4**(10), pp. 759–764.
- [20] Hyun, S., Karlsson, A. M., Torquato, S., and Evans, A. G., 2003, "Simulated Properties of Kagomé and Tetragonal Truss Core Panels," *Int. J. Solids Struct.*, **40**(25), pp. 6989–6998.
- [21] Hutchinson, J. W., and He, M. Y., 2000, "Buckling of Cylindrical Sandwich Shells With Metal Foam Cores," *Int. J. Solids Struct.*, **37**, pp. 6777–6794.
- [22] Bart-Smith, H., Hutchinson, J. W., and Evans, A. G., 2001, "Measurement and Analysis of the Structural Performance of Cellular Metal Sandwich Contruction," *Int. J. Mech. Sci.*, **43**, pp. 1945–1963.
- [23] Fleck, N. A., and Deshpande, V. S., 2004, "Blast Resistance of Clamped Sandwich Beams," *J. Appl. Mech.*, (in press).